

Reverse osmosis pilot plant to produce drinking water in Chanduy community of Santa Elena province- Ecuador

Doménica Urdánigo Bustamante¹, Juan Cedeño Laje¹, Julianny Torres Cano¹, Jonathan Mendez Ruiz, Ing¹, Cindy Goyburo Chávez, Ing¹, Samantha Jiménez Oyola, PhD¹, and Priscila Valverde Armas, PhD¹

¹Escuela Superior Politécnica del Litoral, ESPOL, Faculty of Engineering in Earth Sciences, Campus Gustavo Galindo Km. 30.5 Vía Perimetral, ESPOL Polytechnic University, Guayaquil P.O. Box 09-01-5863, Ecuador, durdanig@espol.edu.ec, juancede@espol.edu.ec, jntorres@espol.edu.ec, jonimend@espol.edu.ec, cgoyburo@espol.edu.ec, sjimenez@espol.edu.ec, prierval@espol.edu.ec

Abstract – Desalination using reverse osmosis (RO) systems is one of the water technologies introduced to address freshwater scarcity in arid and semi-arid regions through the production of water with characteristics for human consumption. The Zapotal River Basin located in Santa Elena, Ecuador, is a semi-arid area, where water demand is greater than available water sources. The objective of this research is to design a decentralized RO system to production of water for consumption purposes, in terms of low salinity content. Therefore, a water sampling campaign was carried out in the study area to identify the communities with the greatest need for water desalination. Additionally, physicochemical water parameters and the analysis of major ions in surface and groundwater samples were measured to design a RO desalination system. An open-source software named “WAVE” was used to determine the removal efficiencies and energy consumption. Synthetic water solutions using NaCl electrical conductivity (EC) concentrations ranging from 3000 to 24000 $\mu\text{S}/\text{cm}$ were used as feed water for the RO technology to simulate the measured EC of the study area. The experimental removal efficiency results were 95.98 and 99.52%, with an energy consumption of 3.90 - 4.58 kWh/m^3 . The energy consumption was optimized by increasing the number of membranes in the RO plant simulation. Finally, the importance of this study lies in designing and proposing a brackish water treatment alternative to assure the availability of water for human consumption and its sustainable management, reaffirming what is stated in SDG 6.

Keywords – Reverse osmosis, Electrical conductivity, Energy consumption, Desalination technology.

I. INTRODUCTION

Freshwater constitutes less than 3% of the global water resources, whereas 97% is provided by the water from oceans, lakes, and seas with high content of dissolved salts [1]. Worldwide water scarcity is expected to intensify in the next 20 years, because of population, economic, and energy consumption growth [2]. Therefore, the identification of non-conventional water catchment sources is a necessity nowadays.

Brackish waters are surface or groundwater sources with a salinity content of between 1 and 25 g/L. Freshwater presents a salinity of less than 1 g/L compared to a salinity of seawater

above 35 g/L [3]. In this line, brackish water is a good alternative for desalination compared to seawater, since its treatment results in lower costs and lower energy demand [4]. Muñoz et al., [5] reported that brackish groundwater saves between 0.69 and 1.3 kg CO₂ eq per m³ compared to seawater, generating a lower environmental impact.

Desalination is a technology introduced to address water scarcity [6], [7], by treating water with high salt content and producing water for drinking and industrial purposes with relatively simple and low-cost processes [6]. For desalination purposes, membranes are essential [7], with reverse osmosis (RO) being one of the most promising pressure-driven membrane techniques today [8].

Over the past 40 years, RO membrane technology has been progressing intensively and at present, it represents 44% of the global desalination production market, with a share of about 80% in desalination plants around the world [9]– [11].

RO plants emerge as an alternative for brackish water treatment to other water desalination techniques, such as multi-stage flash (MSF) desalination and multi-effect distillation (MED), requiring less energy, and lower investment and maintenance costs [11], [12]. RO is widely applied in the removal of salts content, hardness, pathogens, turbidity, synthetic organic compounds, inorganic compounds, pesticides, and many contaminants from water [13].

The performance of the RO technique mainly comprises a semi-permeable membrane where water molecules are transported through the membrane and salts are retained. Such behavior is given by applying pressure above the osmotic pressure value, which allows water to flow out of the solution from higher to lower concentration [14]. The benefits of RO include the low space required for the system, the operational and automation ease of the process [15], and a relatively low cost of water production [16]. Consequently, this technology represents a high potential for application in arid and semi-arid regions, where the provision of fresh water is a significant challenge.

Approximately one-third of the rural population in developing countries live in semi-arid and arid regions [11]. Ecuador has 20% of its surface under arid and semi-arid conditions; most of these drylands are concentrated on the Pacific coast side, especially in the provinces of Manabí and

Digital Object Identifier: (only for full papers, inserted by LACCEI).
ISSN, ISBN: (to be inserted by LACCEI).
DO NOT REMOVE

Santa Elena, where the “Chongón-Colonche” mountain range extends [17].

The Zapotal River watershed is a semi-arid zone in the province of Santa Elena, Ecuador. In this area, water demand is greater than water availability [18]. Precipitation is the main source of water; however, evaporation is greater than precipitation [19], thus the communities living in this area are subjected to water stress. In general, there are frequent drought seasons where the aquifer formations are the only source of water supply "of strictly natural origin" while providing the base flow in the river courses [20].

Addressing the problem of water scarcity in Santa Elena, the Chongón - San Vicente irrigation canal, inaugurated in 2014, was built in response to the need for water suitable for irrigation and human consumption [21]. However, this project failed to meet the water demand.

Currently, an important part of the population of Santa Elena is supplied by groundwater. Nevertheless, the aquifers present various problems due to overexploitation, contamination, and the proximity of the sea, which affects their quality and possible uses.

The deployment of an RO desalination system to solve water scarcity problems in semi-arid and arid regions would reduce the environmental impact on a local and global scale by using brackish water from groundwater and surface sources [22]. In this context, this study aims to design a decentralized brackish water treatment system for drinking water production in the communities of the Zapotal River watershed. This system will assure the water quality, with regards to the salinity concentration for drinking purposes. This study will be conducted by focusing on the removal of electrical conductivity content according to local and international water quality standards and considering the water demand of a growing population.

II. METHODOLOGY

A. Study area

The study area is located in the Zapotal River watershed in the province of Santa Elena, Ecuador (Fig. 1). This watershed is a coastal plateau with plains or semi-undulating plains, with short streams and small, narrow, shallow, and seasonal rivers, which flow into the Pacific Ocean [23], [24]. In this intermittent dendritic drainage watershed, the main rivers are Verde, Azúcar, Seco, Campaña, and San Rafael. These rivers converge to the Zapotal river, the most important tributary since it supplies water to the urban communities [23].

The study area is semi-arid and therefore represents a deficit of surface water sources [24]. According to [25], in this zone, there is scarce precipitation marked with intrannual (torrential) and interannual (droughts) irregularity. According to reports from the National Institute of Meteorology and Hydrology of Ecuador (INAMHI), the average annual precipitation is 264 mm/year, and the average annual temperature is 24.3 °C [26].

Some of the geological formations leading to the formation of local - discontinuous aquifers within the Zapotal River watershed are the San Eduardo Formation, which is formed of limestones; the Ancon, Socorro, and Seca Group Formations and the Dos Bocas Formation, which present secondary formation gypsum; and the Cayo Formation, which contains siliceous lullites and chert. These formation aquifers are porous-free-coastal and are highly related to alluvial deposits, generating suitable conditions for groundwater accumulation. Notably, that groundwater is exploited for the supply of populations in the sectors [27].

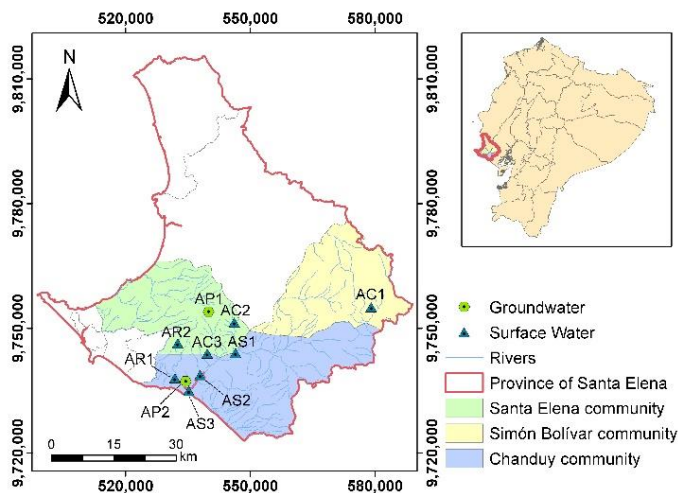


Fig. 1 Map of the study area showing surface and groundwater sampling points in the province of Santa Elena, Ecuador.

B. Sampling and analytical measurements

Ten water samples (n=10) were collected during the dry season of September 2022 in the communities of Chanduy, Santa Elena, and Simón Bolívar. Eight samples corresponded to surface sources and two were from groundwater sources. Samples AS1, AS2, and AS3 were from surface water, sampled in rivers. Samples AR1 and AR2 corresponded to surface water samples, sampled in reservoirs. Samples AC1, AC2, and AC3 were collected at different points of the Chongón - San Vicente irrigation canal. Samples AP1 and AP2 were collected from groundwater (deep wells) in the Saya and Manantial communities (Fig. 1).

Physicochemical water parameters, such as pH, electrical conductivity (EC), total dissolved solids (TDS), and temperature (T) were measured on-site using a HANNAH multiparameter (HI 9829) calibrated against pH and EC standards. Samples were refrigerated and transported following the guidelines of the Ecuadorian standard NTE INEN 2169 [28]. The analysis of major ions as Ca^{2+} , Mg^{2+} , Na^+ , K^+ , Cl^- , SO_4^{2-} , HCO_3^- , NO_3^- and NO_2^- was performed at the Sanitary Laboratory of the Escuela Superior Politécnica del Litoral (ESPOL).

Ca^{2+} and Mg^{2+} concentrations were determined by volumetric titration with EDTA. HCO_3^- concentration was

measured by titration with sulfuric acid. The Na^+ ion was analyzed by potentiometry (HACH probe). The other major ions were analyzed with visible light spectrophotometry using the HACH DR 3900 equipment. Verification with the standards for adjustment was performed before each measurement of major ions.

C. Experimental procedure

The desalination process was carried out in the reverse osmosis pilot plant shown in Fig. 2. Synthetic water was prepared by dissolving table salt (NaCl) in the feed tank to obtain different EC concentrations ranging from 3000 to 24000 $\mu\text{S}/\text{cm}$ (increasing 3000 $\mu\text{S}/\text{cm}$ in each experiment). The purpose was to simulate the EC measured in the study area. The RO system has a storage tank where the water is pumped to a multimedia filter by a centrifugal pump (1 hp) to reduce turbidity and solids suspension. The filter column had gravel, zeolite, and activated carbon. The water flowed to the ultraviolet (UV) light cabinet for pathogen inactivation, and subsequently pumped to a filtration process (5 and 1 μm). The water was pumped to the membrane by a high-pressure pump (17 bar). The membrane presented a recovery rate of 15%. To calculate the salinity removal efficiency, the physicochemical parameters EC and TDS were measured. In addition, the HCO_3^- content of the feed water (synthetic water), permeate, and concentrate was monitored.

D. Modelling

To make a comparative analysis of the theoretical and experimental removal efficiencies, TDS removal modeling was performed in the Water Application Value Engine (WAVE, version 1.77) software. The following parameters were input to

the model: permeate flow rate, pH, concentration of major ions (Cl^- y Na^+), turbidity, total organic carbon (TOC), total suspended solids (TSS), and temperature.

Subsequently, to model the reduction in energy consumption, the reverse osmosis plant was simulated by increasing the number of RO membranes and adding recirculation processes.

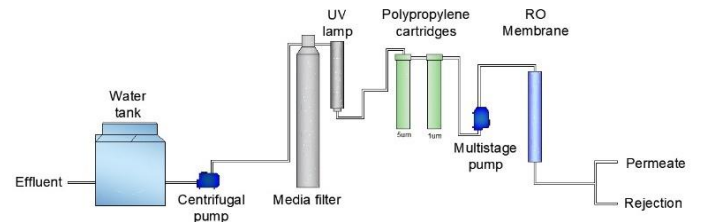


Fig. 2 Schematic diagram of reverse osmosis pilot plant.

III. RESULTS

A. Hydrochemical analysis

Fig. 3 presents the hydro-chemical composition of surface and groundwater in the study area using Stiff diagrams. These diagrams show that most of the groundwater exhibits sodium-chloride hydrochemical composition. For instance, surface water point (AS3) showed concentrations of 500 mEq/L of Cl^- and Na^+ . The remaining surface water samples presented concentrations ranging from 12 to 60 mEq/L of Cl^- , and 12 to 40 mEq/L of Na^+ . The salinity content could be attributed to their proximity to the seashore. Additionally, the sodium-chloride composition is consistent with the groundwater type of AP1 and AP2. Since these wells are deep, water-rock interaction is favored, increasing the salinity of the water [29].

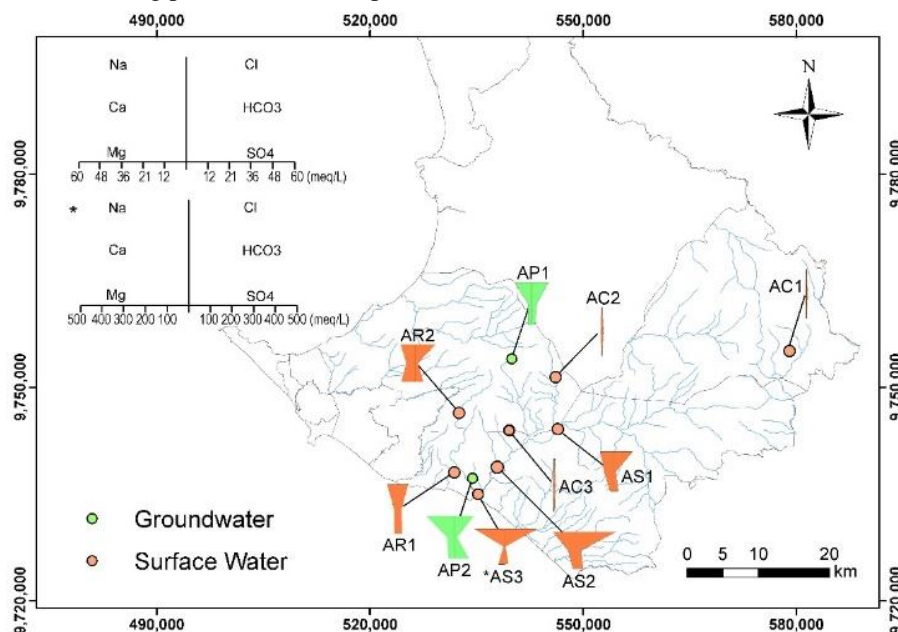


Fig. 3 Stiff diagrams that show the hydro-chemical composition of water samples in the study area of Zapotal. There are two scales, groundwater, and surface water*.

The water of the Chongón-San Vicente irrigation canal was calcium-bicarbonate with concentrations of about 1.5 mEq/L of HCO_3^- and 1 mEq/L of Ca^{2+} . The presence of these ions may result from sedimentary formations (San Eduardo Formation) consisting of hard limestones that interact with surface water [30].

B. Physicochemical characterization of water

The water from the sampling points presented EC values ranging from 109 to 16270 $\mu\text{S}/\text{cm}$, with an average EC of $3102 \pm 4785.42 \mu\text{S}/\text{cm}$ as shown in Table I. It was observed that the pH values of the points studied were alkaline, ranging from 7.32 to 8.84. The most basic pH value corresponded to the surface water sample AS3, it also presented a high TDS concentration of 9460 mg/L. The World Health Organization (WHO) establishes as a recommended limit for EC, a threshold of no more than 800 $\mu\text{S}/\text{cm}$ for drinking water and 500-600 mg/L of TDS [31], [32]. Moreover, according to NTE INEN 1108 [33], water pH for human consumption must meet a threshold between 6.5 and 8.0. Therefore, the study points that require attention, in order of importance according to their critical status, are AR1, AP1, AS1, AR2, AP2, AS2, and AS3. The water sample point, AP2, was the focus of this work since it is a water catchment source used for human consumption.

TABLE I
PHYSICOCHEMICAL PARAMETERS MEASURED IN-SITU.

Type of Source	Sampling point	EC [$\mu\text{S}/\text{cm}$]	TDS [mg/L]	pH	T [$^{\circ}\text{C}$]
Surface water	AC1	109	50	7.32	27
	AC2	136	65	7.29	25
	AC3	146	70	7.75	25
	AR1	1219	564	7.93	28
	AR2	2890	1410	7.57	27
	AS1	2010	1039	7.89	24
	AS2	3250	1709	7.78	24
Groundwater	AS3	16270	9460	8.84	24
	AP1	1916	969	8.51	24
	AP2	3070	1471	7.72	28

C. Desalination experiments

The desalination process was performed using the reverse osmosis pilot plant. Experiments were carried out with synthetic water, obtaining TDS removal efficiency percentages between 95.98 and 99.52%. Table II shows the removal efficiency for each EC concentration scenario. It was demonstrated that the higher the EC in the feed water, the higher the EC of the permeate and reject effluents. For instance, by increasing the EC from 6000 to 18000 $\mu\text{S}/\text{cm}$, the permeate concentration increased from 36.8 to 304.0 $\mu\text{S}/\text{cm}$, respectively. Similar results were reported in [1], employing spiral wound membranes, and varying the salinity of the feed flow between 25 and 45 kg/m^3 , it was found that increasing the salinity concentration of the feed water increased the permeate salinity by 67%, and by 45% in the rejection flow.

It can be observed that the permeate flow rate has a decreasing trend, starting with an average of $1.48 \pm 0.05 \text{ GPM}$

when desalinating 3011.3 $\mu\text{S}/\text{cm}$, and ending with a flow rate $<0.5 \text{ GPM}$ when desalinating 24003.3 $\mu\text{S}/\text{cm}$. This trend leads to a lower permeate volume compared to the concentrate volume. In addition, it was found that the permeate pressure increased by 1.1% as the salt content increased, as well as the concentrate water pressure by 1.5%. This behavior might be associated with the variation in the osmotic pressure required for the water to be treated to flow through the membrane, which implies a higher energy demand and thereafter higher cost in permeate water production [5], [34].

The pilot-scale RO system under the current configuration desalinates water that complies with the WHO standards, i.e., up to an EC concentration of about 800 $\mu\text{S}/\text{cm}$. Even when the feed water is higher than 21000 $\mu\text{S}/\text{cm}$, the EC of the permeate was 528.75 $\mu\text{S}/\text{cm}$, meeting the WHO standards. Communities such as Chanduy-San Rafael (AS2) and Zapotal (AS3), which are supplied by catchment water from the Zapotal River and *Boca Rio Chanduy*, could benefit from this type of advanced water treatment technology.

Table II shows the variation of pH in the water in both the permeate and reject streams. For example, the permeate flow tended to be basic and the reject tended to be acidic. This may be due to the low bicarbonate concentration in the feed water which ranged between 37.25 mg/L and 46.50 mg/L respectively. Low bicarbonate concentrations may be associated with poor buffering capacity, i.e., poor ability to mitigate changes in the proton concentration in water, resulting in alkaline treated water (permeate).

D. Simulation versus experimentation

Theoretical (software) and experimental (pilot plant) TDS removal performance was compared. Fig. 4 shows the experimental and simulation results of TDS concentration removal in the permeate or treated water. The TDS experimental concentrations are lower compared to the simulation results for the permeate. For example, when removing 15000 $\mu\text{S}/\text{cm}$, experimental TDS concentrations of 94 mg/L for permeate and 8265 mg/L for reject are obtained, while the simulation reported 118 and 9927 mg/L TDS, respectively. However, when the TDS concentration exceeded 18000 or 21000 $\mu\text{S}/\text{cm}$, the experimental values were higher than the simulated ones. To exemplify, when the EC was 24000 $\mu\text{S}/\text{cm}$, the experimental TDS were 482 and 123667 mg/L for permeate and concentrate, while the simulation TDS were 295 and 16521 mg/L, respectively. These results show that the reverse osmosis pilot plant under the current configuration efficiently removes ions up to treating water with concentrations of EC of $<21000 \mu\text{S}/\text{cm}$.

Fig. 5 shows the results of the TDS level in the simulated and experimental concentrates when increasing EC levels. The simulated TDS concentrations were higher than the experimental values. This implies that the plant removes less TDS than expected.

TABLE II
EXPERIMENTAL RESULTS OF THE PILOT-SCALE REVERSE OSMOSIS SYSTEM.

Nominal electrical conductivity ($\mu\text{S/cm}$)	Measured electrical conductivity ($\mu\text{S/cm}$)			pH			Pressure (bar)		Flow of permeate (GPM)	Removal efficiency (%)
	Synthetic	Permeate	Concentrate	Synthetic	Permeate	Concentrate	Permeate	Concentrate		
3000	3011.3	14.5 \pm 3.11	3602.3 \pm 267.74	6.76	8.22	6.42	3.6	12.7	1.48	99.52
6000	6008.0	36.8 \pm 4.36	7270.5 \pm 136.86	6.93	9.63	7.52	3.7	13.0	1.28	99.39
9000	9006.0	106.5 \pm 30.16	7270.5 \pm 175.31	5.76	6.79	4.76	3.8	13.6	1.13	98.82
12000	12005.0	180.8 \pm 46.19	13985.0 \pm 336.80	6.64	8.17	6.25	3.8	13.9	0.88	98.49
15000	15005.0	188.3 \pm 7.85	16525.0 \pm 461.92	6.71	8.51	6.66	3.9	13.9	0.69	98.75
18000	18002.5	304.0 \pm 58.29	19295.0 \pm 562.70	6.45	7.50	6.16	3.9	14.6	0.53	98.31
21000	21002.5	528.8 \pm 64.97	21772.3 \pm 496.95	6.56	7.65	6.31	3.7	13.7	<0.50	97.48
24000	24003.3	964.7 \pm 135.68	24733.3 \pm 122.20	6.64	8.17	6.25	3.8	14.0	<0.50	95.98

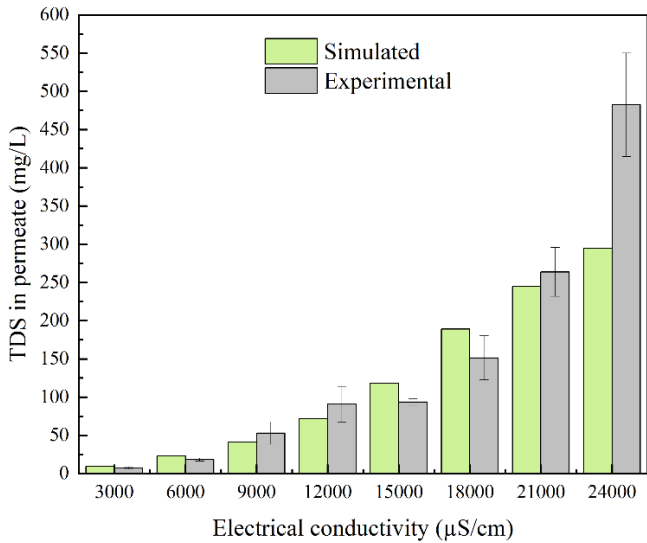


Fig. 4 Results of the TDS value of the permeate (treated water) at different conductivity concentrations.

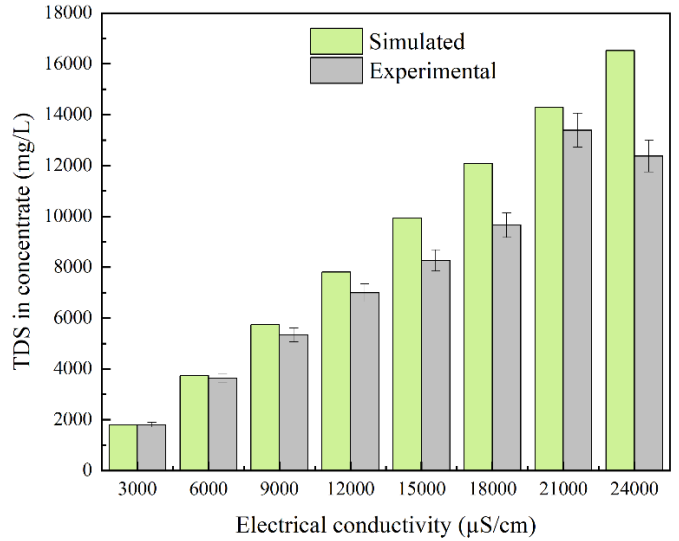


Fig. 5 Results of the TDS of the concentrate at different electrical conductivity concentrations.

E. Energy consumption

Fig. 6 presents the energy consumption for each EC concentration to be decreased. The energy consumption, resulting from the simulation, varies between 3.90 and 4.58 kWh/m^3 when the EC of the water varied between 3000 and 24000 $\mu S/cm$. These results demonstrate that an RO system under the current design could use the same amount of energy to treat water with a salinity concentration of 3000 $\mu S/cm$ compared to treating water with an EC of 21000 $\mu S/cm$. This highlights that the RO treatment system is less energy efficient for treating water with low EC. Considering the high energy consumption of the RO process [4], it was crucial to reduce it to make the deployment of this type of technology feasible in communities with limited economic resources and without access to drinking water.

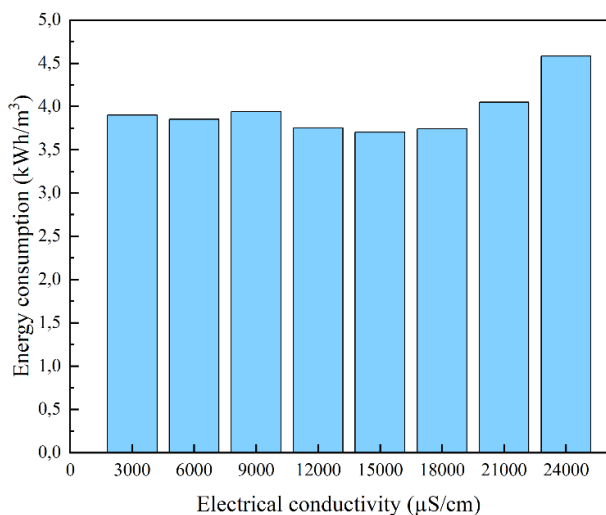


Fig. 6 Energy consumption as a function of increasing conductivities in feed water.

Fig. 7 shows the schematic of the RO system to reduce energy consumption at increasing EC concentrations. To achieve this, more membranes were incorporated in a series set-up to increase the recovery percentage of the designed plant (Table III). In addition, there was a designated recirculation flow rate for each type of concentration, thereby increasing the percentage of recovery and thus obtaining a greater volume of permeate. This resulted in energy savings and an increase in the volume of water that can be treated.

TABLE III

RESULTS OF THE NEW REVERSE OSMOSIS PLANT SET-UP, RECOVERY OF 55%

Nominal EC ($\mu S/cm$)	Stage1 memb	Stage2 memb	Optimized energy (kWh/m^3)	TDS (mg/L)	Energy saving (%)
3000	4	0	0.74	19.8	81.0
6000	4	0	0.95	42.9	75.3
9000	4	0	1.25	103.6	68.3
12000	3	2	1.33	154.6	64.5
15000	4	3	1.22	165.6	67.0
18000	4	3	1.33	291.0	64.4
21000	4	4	1.45	415.6	64.2
24000	5	5	1.52	630.5	63.4

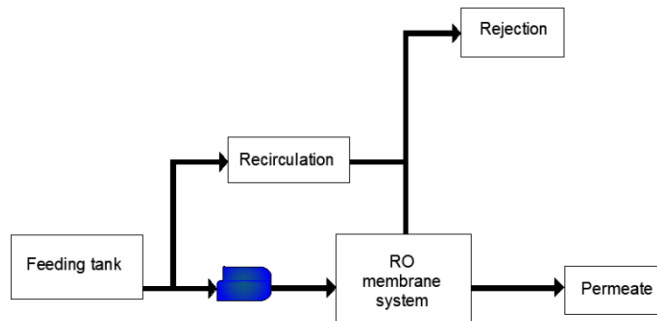


Fig. 7 Scheme of reverse osmosis plant to optimize energy consumption.

Table III reports that with the optimized RO system set-up, the energy consumption was reduced to 0.74 kWh/m^3 for treating brackish water with an EC value of 3000 $\mu S/cm$, and decreased to 1.52 kWh/m^3 for treating water with an EC of 24000 $\mu S/cm$. This optimization leads to energy savings of 81.0, 67.0, and 63.4 % for treating water with EC of 3000, 15000, and 24000 $\mu S/cm$, respectively.

IV. CONCLUSIONS

Most of the groundwater sources being monitored in the Zapotal River Basin present sodium-chloride hydrochemical facies due to the mineralogical characteristics of the watershed geological formation. It was identified that the water from the communities of Chanduy, Manantial, Zapotal, and Saya presented EC in a range of 109 to 16270 $\mu S/cm$, therefore, this research proposes a decentralized reverse osmosis system to desalinate the water until it reaches the EC concentration of 800 $\mu S/cm$ suggested by the WHO for consumption purposes.

RO treatment allowed the removal of salts with an efficiency of 95.98 to 99.52%. According to the results, the current RO plant configuration (single pass, one stage) effectively desalinates brackish water at concentrations of approximately 21000 $\mu S/cm$.

The current system presented a high energy consumption (3.90-4.58 kWh/m^3), hence a new configuration was proposed in the RO system in which the number of membranes was increased, reaching a reduction of energy consumed of 81.0 % to desalinate water with EC of 3000 $\mu S/cm$ and 63.4 % for 24000 $\mu S/cm$. This could improve the efficiency of treatment to be efficient in terms of desalination and energy consumption and be applied in communities with scarce water availability.

ACKNOWLEDGMENT

The authors acknowledge the support of the Faculty of Earth Sciences Engineering (FICT) of the Escuela Superior Politécnica del Litoral (ESPOL) for funding this project.

REFERENCES

- [1] S. H. Aladwani, M. A. Al-Obaidi, and I. M. Mujtaba, "Performance of reverse osmosis based desalination process using spiral wound membrane: Sensitivity study of operating parameters under variable seawater conditions," *Clean Eng Technol*, vol. 5, Dec. 2021, doi: 10.1016/j.clet.2021.100284.
- [2] S. Chu et al., "Experimental Study on the Influence of Flexible Control on Key Parameters in Reverse Osmosis Desalination," *IEEE Access*, vol. 10, pp. 4844–4860, 2022, doi: 10.1109/ACCESS.2021.3140071.
- [3] J. R. Du, X. Zhang, X. Feng, Y. Wu, F. Cheng, and M. E. A. Ali, "Desalination of high salinity brackish water by an NF-RO hybrid system," *Desalination*, vol. 491, Oct. 2020, doi: 10.1016/j.desal.2020.114445.
- [4] H. Shemer and R. Semiat, "Sustainable RO desalination – Energy demand and environmental impact," *Desalination*, vol. 424. Elsevier B.V., pp. 10–16, Dec. 15, 2017. doi: 10.1016/j.desal.2017.09.021.
- [5] I. Muñoz and A. R. Fernández-Alba, "Reducing the environmental impacts of reverse osmosis desalination by using brackish groundwater resources," *Water Res*, vol. 42, no. 3, pp. 801–811, 2008, doi: 10.1016/j.watres.2007.08.021.
- [6] D. E. Sachit and J. N. Veenstra, "Analysis of reverse osmosis membrane performance during desalination of simulated brackish surface waters," *J Memb Sci*, vol. 453, pp. 136–154, Mar. 2014, doi: 10.1016/j.memsci.2013.10.051.
- [7] E. Hosseinipour, K. Park, L. Burlace, T. Naughton, and P. A. Davies, "A free-piston batch reverse osmosis (RO) system for brackish water desalination: Experimental study and model validation," *Desalination*, vol. 527, Apr. 2022, doi: 10.1016/j.desal.2021.115524.
- [8] G. Amy et al., "Membrane-based seawater desalination: Present and future prospects," *Desalination*, vol. 401, pp. 16–21, Jan. 2017, doi: 10.1016/j.desal.2016.10.002.
- [9] M. J. Kotelyanskii, N. J. Wagner, and M. E. Paulaitis, "Atomistic simulation of water and salt transport in the reverse osmosis membrane FT-30," 1998.
- [10] H. F. Ridgway, A. Kelly, C. Justice, and B. H. Olson, "Microbial Fouling of Reverse-Osmosis Membranes Used in Advanced Wastewater Treatment Technology: Chemical, Bacteriological, and Ultrastructural Analyses," 1983. [Online]. Available: <https://journals.asm.org/journal/aem>
- [11] A. Zapata-Sierra, M. Cascajares, A. Alcayde, and F. Manzano-Agugliaro, "Worldwide research trends on desalination," *Desalination*, vol. 519. Elsevier B.V., Jan. 01, 2022. doi: 10.1016/j.desal.2021.115305.
- [12] J. Salazar, F. Tadeo, and C. Prada, "Renewable energy for desalination using reverse osmosis," *Renewable Energy and Power Quality Journal*, vol. 1, no. 8, pp. 1229–1234, Apr. 2010, doi: 10.24084/repqj08.631.
- [13] A. Ruiz Martínez and M. Coronado Coronel, "Tratamiento de agua subterránea mediante la utilización de ósmosis inversa para consumo familiar en el sector Chuina, Morales-San," *revista ciencia, tecnología y desarrollociencia, tecnología y desarrollo*, vol. 2, no. 2313–7991, pp. 7–16, 2016. [Online]. Available: https://revistas.upeu.edu.pe/index.php/ri_ctd/article/view/621
- [14] S. S. Shenvi, A. M. Isloor, and A. F. Ismail, "A review on RO membrane technology: Developments and challenges," *Desalination*, vol. 368. Elsevier B.V., pp. 10–26, Jul. 15, 2015. doi: 10.1016/j.desal.2014.12.042.
- [15] M. Qasim, N. N. Darwish, S. Mhiyo, N. A. Darwish, and N. Hilal, "The use of ultrasound to mitigate membrane fouling in desalination and water treatment," *Desalination*, vol. 443. Elsevier B.V., pp. 143–164, Oct. 01, 2018. doi: 10.1016/j.desal.2018.04.007.
- [16] P. K. Park, S. Lee, J. S. Cho, and J. H. Kim, "Full-scale simulation of seawater reverse osmosis desalination processes for boron removal: Effect of membrane fouling," *Water Res*, vol. 46, no. 12, pp. 3796–3804, 2012, doi: 10.1016/j.watres.2012.04.021.
- [17] Ricardo Ayerza, "Importancia hídrica de los bosques de la cordillera Chongón- Colonche para las tierras áridas del noroeste de Santa Elena," 2019. Accessed: Feb. 01, 2023. [Online]. Available: <https://revistas.unl.edu.ec/index.php/bosques/article/view/582/522>
- [18] H. M. Summers and J. C. Quinn, "Improving water scarcity footprint capabilities in arid regions through expansion of characterization factor methods," *Science of the Total Environment*, vol. 801, Dec. 2021, doi: 10.1016/j.scitotenv.2021.149586.
- [19] A. Mostafaiepour, S. M. Mohammadi, F. Najafi, and A. Issakhov, "Investigation of implementing solar energy for groundwater desalination in arid and dry regions: A case study," *Desalination*, vol. 512, Sep. 2021, doi: 10.1016/j.desal.2021.115039.
- [20] A. Jodar-Abellan, M. Ruiz, and J. Melgarejo, "Evaluación del impacto del cambio climático sobre una cuenca hidrológica en régimen natural (SE, España) usando un modelo SWAT," *Revista Mexicana de Ciencias Geológicas*, vol. 35, no. 3, pp. 240–253, 2018, doi: 10.22201/cgeo.20072902e.2018.3.564.
- [21] Diego Noboa, "Diagnóstico de las fuentes de salinidad para identificar el comportamiento hidrológico e hidroquímico a lo largo del canal de riego Chongón-San Vicente," *ESCUELA SUPERIOR POLITÉCNICA DEL LITORAL*, Guayaquil, 2021.
- [22] E. H. Alali, "Groundwater history and trends in Kuwait," *WIT Transactions on Ecology and the Environment*, vol. 112, pp. 153–164, 2008, doi: 10.2495/SI080161.
- [23] Mora Daniella, "Evaluación del Balance sedimentario de las Cuencas Hidrográficas de Zapotal y Jipijapa hacia la zona litoral," Guayaquil, 2021.
- [24] I. García-Garizábal, P. Romero, S. Jiménez, and L. Jordá, "Climate change effects on the climate dynamics of Coastal Ecuador," *DYNA (Colombia)*, vol. 84, no. 203, pp. 37–44, Dec. 2017, doi: 10.15446/dyna.v84n203.59600.
- [25] M. B. Bernabé-Crespo, "Implicaciones y perspectivas del mix hídrico para el abastecimiento de agua potable en el sureste de España," *Agua y Territorio / Water and Landscape*, no. 20, p. e5714, Feb. 2022, doi: 10.17561/at.20.5714.
- [26] INAHMI, "ANUARIO METEOROLÓGICO," 2015.
- [27] Rodríguez Carlos and Astudillo Leonardo, "CARACTERIZACIÓN HIDROGEOLÓGICA DE LAS CUENCAS DE LOS RÍOS JAVITA Y ZAPOTAL DE LA PENINSULA DE SANTA ELENA," *Universidad Central del Ecuador, Quito*, 2014.
- [28] NTE INEN 2169, "AGUA. CALIDAD DEL AGUA. MUESTREO. MANEJO Y CONSERVACIÓN DE MUESTRAS." 2013.
- [29] M. Melo and E. Carol, "Variaciones geomorfológicas como condicionantes de la química del agua subterránea en el litoral del estuario medio del Río de la Plata," *Revista del Museo de La Plata*, vol. 5, no. 2, pp. 475–485, Aug. 2020, doi: 10.24215/25456377e120.
- [30] García Yoandris, Balmaseda Carlos, and Varga Heriberto, "Caracterización hidroquímica de las aguas de riego de la cuenca del río Naranjo, municipio Majibacoa, provincia Las Tunas," *Revista Ciencias Técnicas Agropecuarias*, vol. 21, no. 3, pp. 29–34, Jul. 2012.
- [31] S. Indika et al., "Evaluation of performance of existing ro drinking water stations in the north central province, sri lanka," *Membranes (Basel)*, vol. 11, no. 6, Jun. 2021, doi: 10.3390/membranes11060383.
- [32] Truque Paola, *ARMONIZACION DE LOS ESTANDARES DE AGUA POTABLE EN LAS AMERICAS PAOLA ANDREA TRUQUE B.* 2015. Accessed: Feb. 02, 2023. [Online]. Available: <https://www.oas.org/dsd/publications/classifications/Armoniz.EstandaresAguaPotable.pdf>
- [33] SERVICIO ECUATORIANO DE NORMALIZACIÓN, "NTE INEN 1108. AGUA PARA CONSUMO HUMANO. REQUISITOS." 2011.
- [34] H. Khaled, K. Hidouri, and B. Chaouachi, "HYBRID DESALINATION COMBINING MICROBIAL CELLS AND REVERSE OSMOSIS," *JP Journal of Heat and Mass Transfer*, vol. 26, pp. 179–196, Apr. 2022, doi: 10.17654/0973576322019.